INDONESIAN JOURNAL ON GEOSCIENCE
Geological Agency
Ministry of Energy and Mineral Resources

Journal homepage: https://ijog.geologi.esdm.go.id
ISSN 2355-9314, e-ISSN 2355-9306

Hydrogeochemistry and Groundwater Quality Assessment of Shallow Groundwater in the Penguluran Basin, East Java, Indonesia

Ferryati Masitoh[1], Alfi Nur Rusydi[2], and Didik Taryana[1]

[1]Department of Geography, Universitas Negeri Malang, Jln. Semarang 5, Malang City, Indonesia
[2]Department of Information System, Universitas Brawijaya, Jln. Veteran, Malang City, Indonesia

Corresponding Author: ferryati.masitoh.fis@um.ac.id
Manuscript received: January, 05, 2024; revised: April, 28, 2025;
approved: September, 24, 2025; available online: October, 14, 2025

Abstract - Research of the hydrogeochemistry and groundwater quality of shallow groundwater in the Penguluran Basin, East Java, Indonesia, is still very limited. This study aims to identify hydrogeochemistry and groundwater quality in the shallow groundwater of the Penguluran Basin. Twelve water samples were taken from the residents' wells in July during the dry season. Groundwater samples were analyzed in the laboratory to determine the concentration of major ions. The major ions, including Mg^{2+}, Na^{+}, K^{+}, Ca^{+} and anion CO_3^{2-}; HCO_3^{-}; SO_4^{2-}; Cl^{-}. Laboratory results were analyzed using Piper Trilinear Diagram and Gibbs Diagram, Weathering type, Sodium Adsorption Ratio (SAR), Soluble Sodium Percentage (SSP), Residual Sodium Carbonate (RSC), Permeable Index (PI), Magnesium Hazard (MH), Chloro-Alkaline Indices (CAI), Corrosivity Ratio (CR), and Anthropogenic Impact (AI) using NO_3^{-}. The results showed that hydrogeochemical facies in the studied area were of Ca^{+}- Mg^{2+}- HCO_3^{-} type. Groundwater cations were dominated by Ca^{+}, while anions were dominated by HCO_{3-}. The concentration of cations were $Ca^{+} > Mg^{2+} > Na^{+} > K^{+}$, while the anions were $HCO_{3-} > Cl^{-} > SO_4^{2-} > CO_3^{2-}$. Groundwater in Penguluran Basin was freshwater with silicate weathering type. Analysis of major groundwater ions for agricultural irrigation purposes showed that most groundwater samples were safe for agricultural irrigation. CAI-I and CAI-II had mostly negative values. Samples showing negative CAI values also showed silica weathering. CR values were mostly <1 indicated that naturally groundwater was safe from corrosive vulnerability for industry purposes. Nitrate levels in the groundwater showed that 58 % exceeded the allowable limit due to the high risk of anthropogenic impacts to groundwater. The research is expected to provide new information about groundwater in the Penguluran Basin.

Keywords: hydrogeochemistry, groundwater quality, shallow groundwater, Penguluran Basin

How to cite this article:
Masitoh, F., Rusydi, A.N., and Taryana, D., 2025. Hydrogeochemistry and Groundwater Quality Assessment of Shallow Groundwater in the Penguluran Basin, East Java, Indonesia. *Indonesian Journal on Geoscience*, 12 (3), p.343-365. DOI: 10.17014/ijog.12.3.343-365

Introduction

Background

The Java Island has a large number of people population in Indonesia (BPS, 2019), so the groundwater is more needed than in other islands. The highest groundwater needs are in big cities and industrial cities (Marganingrum, 2018; Taufiq *et al*., 2018; Bremard, 2022). However, groundwater information had not yet been evenly distributed in various regions in Java, including Penguluran Basin, South Malang, that were in East Java Province, Indonesia. Until now, there are still limited research about groundwater conditions in the basin (Juwono *et al*., 2022), especially regarding the groundwater quality.

The Penguluran Basin is primarily used for agricultural land, including forestry, sugarcane

plantations, paddy fields, mixed gardens, and agroforestry (Figure 1a). Intensive agricultural areas like paddy fields are only found near the estuary, irrigated from the Penguluran River. Other agricultural lands utilize rainwater or dug wells for groundwater. For nonagricultural purposes, residents solely rely on shallow groundwater to meet their needs. Residents create traditional shallow dug wells close to their homes or agricultural lands (Figure 1b). The groundwater is then pumped and distributed through a pipe network, and used by several households.

Groundwater is the main source for fulfilling water needs in The Penguluran Basin. The increasing population in this area requires a large amount of water (Arifianto, 2016; BPS, 2019), as well as varying geological conditions, which necessitate a comprehensive study, especially on its groundwater quality (Heru and Prasetia, 2024; Rositha *et al*., 2024). Groundwater quality encompasses hydrogeochemical facies and groundwater quality in Penguluran Basin (Poetra *et al*., 2020). This study aims to identify hydrogeochemical facies to assess the groundwater quality in Penguluran Basin. This research is expected to provide comprehensive information of groundwater quality in Penguluran Basin. This research provides novelty in the form of hydrogeochemical and shallow groundwater quality analyses in Penguluran Basin. To date, research in Penguluran Basin has been more related to disaster conditions and its lithological conditions (Arifianto, 2016; Yuwanto and Ridwan, 2017; Utama *et al*., 2020; Heru and Prasetia, 2024). Thus, this study offers a comprehensive overview of the hydrogeochemical conditions and water quality, particularly for its shallow groundwater.

Literature Review

Geological conditions greatly determine the groundwater quality (Sefie *et al.*, 2015). The groundwater quality in the mountains was different compared to that in plain areas (Gibrilla *et al*., 2010). Hydrogeochemistry is an analysis of the interaction between groundwater and its environmental conditions, therefore it can distinguish the groundwater quality (Sefie *et al*., 2015; Egbueri *et al*., 2021; Yuan *et al*., 2022).

The hydrogeochemistry of groundwater had been widely researched to determine the groundwater quality for a lot of purposes (Ghalib, 2017; Asadi *et al*., 2020). Research of groundwater hydrogeochemistry, plays an important role in the identification process of groundwater for agricultural irrigation (Ghalib, 2017; Vasilache *et al.*, 2020), groundwater pollution, and its risks to human health (Zhang *et al*., 2019), and the identification of geological processes and structures that affect groundwater (Li *et al*., 2015; Bouderbala, 2020). Hydrochemical groundwater conditions are shown by several chemical groundwater parameters which included pH, electrical conductivity (EC), salinity, major anions, and cations (Ghalib, 2017). The hydrochemistry of groundwater is influenced by many factors. The water movement in the water cycle also affects groundwater, which includes precipitation,

Figure 1. (a). Mixed garden near sugarcane plantation, and (b). Traditional shallow dug well in Sumberagung Village.

evaporation, cation exchange, mineral disassociation in geological structures, and water-pollutants mixed with human activities, agriculture, and various biological activities (Appelo and Postma, 1993). Hydrogeochemical facies were related to the leaching and rocks weathering process (Xu and Su, 2019). Hydrogeochemichal facies were a classification of major chemical compositions presented in Piper, Durov, Kurlov, Gibbs, and Schoeller Diagram. Those diagram would show the hydrogeochemical group of groundwater facies based on the dominant element of the groundwater chemical major compositions (Jankowski, 2000).

Previous studies have extensively focused on hydrogeochemical facies, using various diagrams to classify groundwater quality such as Piper; Durov (Razi *et al*., 2024) and Gibbs (Poetra *et al*., 2020; Razi *et al*., 2024; Suhendar *et al.*, 2020). Piper diagrams are most commonly used to examine hydrogeochemical facies and to explain the interactions between water and rocks naturally (Razi *et al*., 2024). Hydrogeochemical research using radioisotopes has also been used in previous researches, for example in structural areas (fault and fold system) (Suhendar *et al.*, 2020) and karst (Setiawan *et al*., 2020). However, overall, the study did not explain water quality specifically such as Sodium Adsorption Ratio (SAR), Soluble Sodium Percentage (SSP), Residual Sodium Carbonate (RSC), Permeable Index (PI), Magnesium Hazard (MH), Chloro-Alkaline Indices (CAI), Corrosivity Ratio (CR), and Anthropogenic Impact (AI). All of these groundwater quality parameters will be appropriate for use in areas dominated by agriculture (Hwang *et al*., 2017). This study offers a comprehensive explanation of groundwater conditions, particularly focusing on hydrogeochemical facies and groundwater quality within The Penguluran Basin.

Geological and Hydrogeological Setting

Penguluran Basin is in Malang Regency, East Java, Indonesia. This area is about 16,802 km^2, located at elevation of 0 – 715 m from the mean sea level. This region belongs to the southern mountainous zone, characterized by its Tertiary volcanic origins (Bemmelen, 1949). The Penguluran Basin has six geological formations: namely, Mandalika (Tomm), Nampol (Tmn), Wuni (Tmw), Wonosari (Tmwl), Tuff Mandalika (Tomt), and Swamps and Rivers Sediment (Qas) (Geological Agency of Indonesia, 2010) (Figure 2). The Mandalika Formation (Tomm) consists of volcanic geological materials including andesite, basaltic, trachyitic, dacitic lava, and propylitized andesitic breccia. These rocks have undergone extensive alterations (Yuwanto and Ridwan, 2017; Heru and Prasetia, 2024). The Nampol Formation (Tmn) is dominated by clastic sedimentary material and tuff sandstone. Its rocks consist of tuffaceous or calcareous sandstone, black claystone, and sandy marl. Iron oxides and gypsum sheets are sometimes also present. This formation provides good groundwater aquifer conditions (Sukadana and Indrastomo, 2011). The Wuni Formation (Tmw) consists of andesite-basalt breccia and lava, tuff breccia, lava breccia, and sandy tuff. The Wonosari Formation (Tmwl) consist of limestone, calcareous sandstone, sandy marl, and claystone intercalations (Juwono *et al.*, 2022). The Mandalika Tuff consists of andesitic-rhyolitic-dacitic tuff, and pumiceous tuff breccia. The Mandalika Tuff (Tomt) and Mandalika Formation underly the Wonosari Formation, while the swamps and river deposits units are located along the downstream to the Penguluran Basin estuaries (Poespowardoyo, 1975). The swamp and river sediment (Qas) formation consists of gravel, sand, clay, and plant remains. The groundwater conditions of each geological formation were different due to the interaction between geological conditions and the surrounding environment. All geological formations were formed on the tertiary lithological layer, except swamp and river deposits which formed during the quaternary period. Based on The Indonesian Hydrogeological Maps, Penguluran aquifers had medium to high productivity, but limited for aquifers formed by cracks, gaps, fracturing, and ducts. The area is dominated by rocks of bedded reef limestone with varying degrees of karstification by hitchhiking over other geological formations. Groundwater potential was small and scarce in the

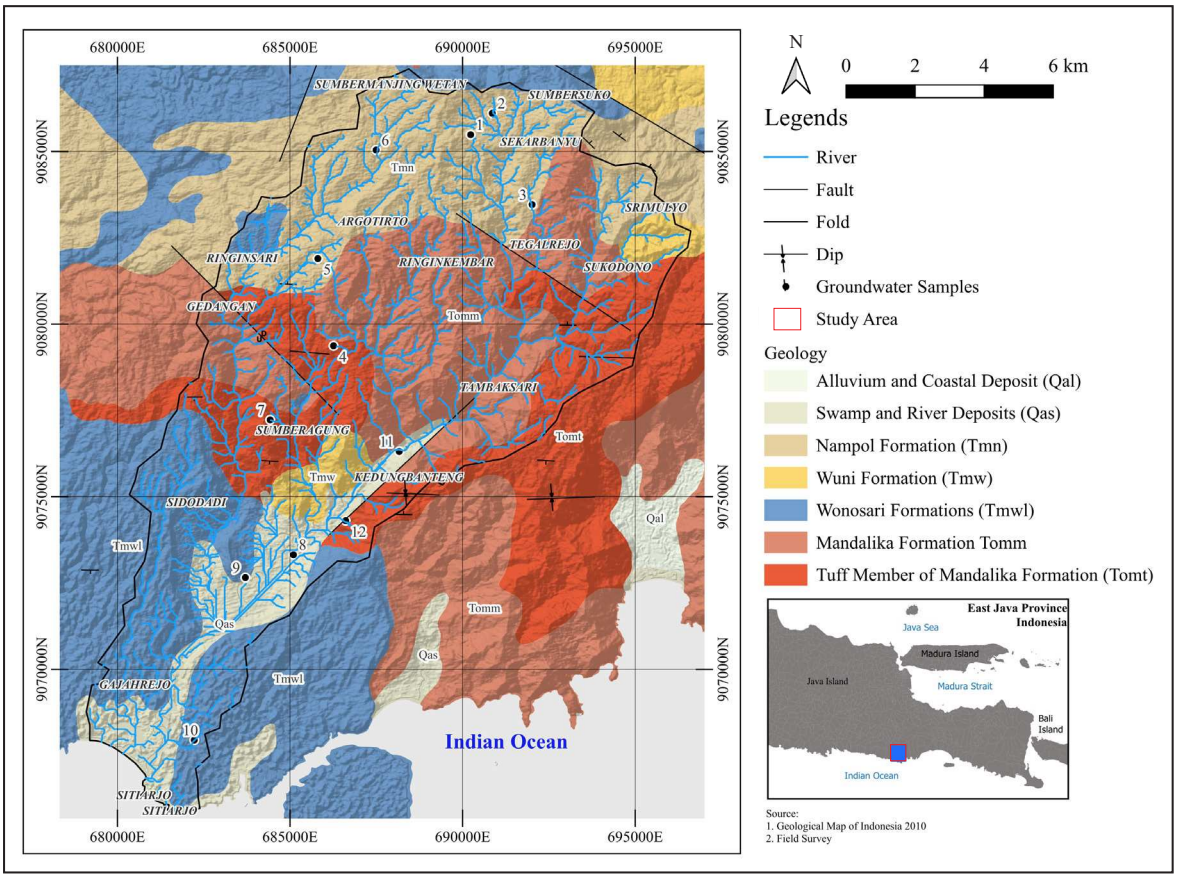

Figure 2. Penguluran geological map and groundwater sample distribution.

aquifers of northern and central basins. Aquifers were dominated by andesite lava flows. Local aquifer which had moderate productivity was in a small percentage area of the Penguluran Basin (Poespowardoyo, 1975).

Naturally, groundwater quality can be influenced by the interaction between rocks and groundwater (hydrogeochemistry), or the input of other substances, for instance due to biological activity and pollution (Gonzales Amaya *et al*., 2019; Yuan *et al*., 2022; Sun and Liu, 2023). The interaction process between groundwater begins with rock weathering. Rock weathering processes can occur physically, chemically, and biologically. Minerals contained within weathered rocks then undergo a dissolution process (Zamroni *et al*., 2022). In limestone, weathering leads to dissolution, which adds Ca^{2+}, Mg^{2+}, SO_4^{2-}, HCO_3^-, and Cl^- ions into groundwater (Mujib *et al*., 2024; Soro *et al*., 2019). The type of rock-forming mineral and its weathering conditions would determine the magnitude of the ions dissolved in the water (Gibrilla *et al*., 2010; Hussien and Faiyad, 2016). Groundwater in the shallow aquifer basin was freshwater. Freshwater occurred due to the weathering process which had the characteristics of high HCO_3^- and low Cl^- (Zhi *et al*., 2021). Groundwater with weathering process also had the characteristics of Na^+/ HCO_3^- (<1), Mg^{2+}/ Ca^{2+} (<1), and Ca^{2+}/ Cl^- (>0.4). Identification of the weathering type could be known through $HCO_3^-+SO_4^{2-}$ and $Ca^{2+}+Mg^{2+}$ (Kaur *et al*., 2017).

Geomorphological Setting

Figure 3 shows the landform map of Penguluran Basin. The studied area has five landform units: River Valley (Ls-V), Denudational Hills (1D-Iblp), Denudational Mountains (2D-Iblp), Karst Solutional Plain (2k-IIsk), and Karst Solutional Hills (3k-IIsk). The River Valley unit is influenced by the Penguluran River System, which has alluvial river deposits. The Denu-

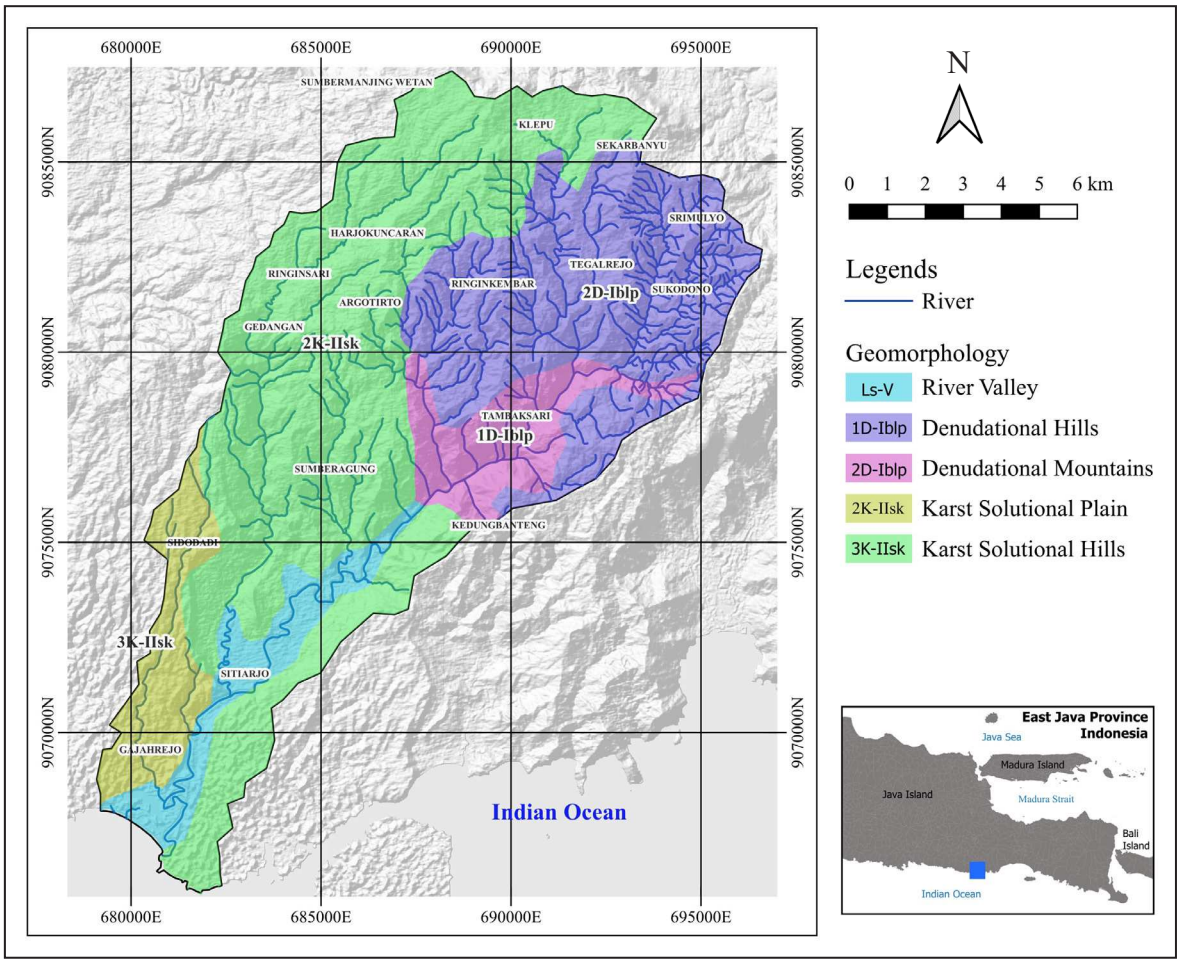

Figure 3. Landform map of Penguluran Basin.

dational Hill Unit (1D-Iblp) and Denudational Mountain Unit (2D-Iblp) are areas that experience intensive erosion and weathering. Geologically, these areas feature andesitic basaltic volcanic rocks. The Karst Solutional Units in the studied area consist of Karst Solutional Plain (2k-IIsk) and Karst Solutional Hills (3k-IIsk). Both of these areas have karst landscapes, but possess different topographical conditions.

Methods and Materials

Groundwater Sampling and Laboratory Analyses

Groundwater sampling considered local hydrogeological conditions. The number of groundwater samples taken were twelve samples located around residential areas. Groundwater samples were tested in-situ and through laboratory analyses. Samples were taken in July 2022, in the dry season on a sunny day. In-situ groundwater samples were tested using a Multi-parameter Water Quality Checker for twelve traditional shallow dug wells. In-situ testing included type of water body (well and spring), Electrical Conductivity (EC), and Turbidity. Water samples were stored in glass bottles equipped with secure lids. The quantity of water samples was determined based on the distribution of geological formations (Figure 2). For wells with pumps, water was pumped out and its quality measured while flowing. For wells without pumps, water was collected using a bucket, and then its quality was measured. After in-situ measurements, the water was subsequently stored in sample bottles. Groundwater samples were also analyzed in the laboratory to obtain major chemical components that included cation

Mg^{2+}, Na^{+}, K^{+}, Ca^{2+}, and anion CO_3^{2-} ; HCO_3^{-}; SO_4^{2-} ; Cl^{-}.

Charge Balance Error (CBE) was used to analyze standard errors from laboratory analysis. The ideal CBE is close to 0 (Li *et al*., 2016). The CBE value used Equation 1. If the CBE value was ± 5 %, then the results of laboratory analysis were acceptable/reliable (Poetra *et al.*, 2020; Tiwari *et al.,* 2020)

$$CBE = \left(\frac{\sum Kation - \sum Anion}{\sum Kation + \sum Anion}\right) * 100\% \quad .....(1)$$

CBE values were calculated using cation and anion levels in meq/L. CBE values of each sample varied between -0.1 and 0.36. The CBE value of all samples is 0.12 which indicates that all samples taken are reliable (Table 1).

Data Analysis

Laboratory results of groundwater samples were analyzed based on major ions (Gibrilla *et al*., 2010). Water quality in this study also included water quality analysis for agricultural irrigation, Chloro-Alkaline Indices (CAI), Corrosivity Ratio (CR), and Anthropogenic Impact to groundwater. Water quality for irrigation included Sodium Adsorption Ratio (SAR), Soluble Sodium Percentage (SSP), Residual Sodium Carbonate (RSC), Permeable Index (PI), Magnesium Hazard (MH) (Hwang *et al*., 2017). ACAI was commonly used by many studies to determine the degree of ion exchange reactions between groundwater and aquifer minerals (Schoeller, 1977; Li *et al*., 2018; Singh *et al*., 2020). CR was used to determine the groundwater susceptibility to corrosive risks based on its major ions (Rout and Setia, 2018; Ram *et al*., 2020). Anthropogenic impact to groundwater used proper nitrate levels for the identification of groundwater pollution (Re *et al*., 2017; Zhang *et al*., 2019).

Analysis of groundwater chemistry data used several parameters (see equation 2−9), and the Piper Trilinear Diagram and Gibbs Diagram. The Piper Trilinear Diagram was very well used for determination of hydrogeochemical groundwater facies (Li *et al*., 2015; Zhi *et al*., 2021), and physicochemical analyzes (Vasilache *et al*., 2020). Gibbs Diagram was used to determine the rock weathering rates (Hwang *et al*., 2017). The composition of groundwater would provide information of the interaction between groundwater and rocks, aquifer conditions, rock weathering, and groundwater recharge quality (Wilopo *et al*., 2020).

Table 1. Major Ion Concentration (K^{+}, Na^{+}, Mg^{2+}, Ca^{2+}, HCO_3^{-}, SO_4^{2-}, Cl^{-})

ID	Location		Kation (meq/l)				Anion (meq/l)			CBE
	X	Y	Ca	Mg	Na	K	HCO3	Cl	SO4	
1	690213	9085443	1.203	0.716	0.422	0.320	0.944	0.643	0.747	0.07
2	690868	9086217	2.156	0.082	0.461	0.430	3.570	0.112	0.005	-0.08
3	691971	9083417	1.517	1.284	0.461	0.977	3.065	0.505	0.487	0.02
4	686311	9079395	1.118	0.239	<0.012	0.340	1.301	0.307	0.285	-0.05
5	685715	9081868	5.190	1.522	0.109	0.818	5.710	0.587	1.722	-0.02
6	687502	9084966	2.395	0.321	< 0.012	0.330	3.275	0.280	0.194	-0.10
7	684434	9077250	5.749	0.239	0.278	0.489	4.954	0.392	1.572	-0.01
8	685059	9073393	4.072	0.560	0.200	0.151	4.997	0.280	0.341	-0.06
9	683778	9072588	6.707	0.716	0.622	< 0.112	2.519	0.784	0.456	0.36
10	682229	9067926	2.076	0.477	0.461	1.476	2.519	0.756	0.685	0.06
11	688098	9076372	1.677	0.477	0.252	0.389	2.435	0.307	0.173	-0.02
12	686608	9074316	2.874	0.403	0.400	0.619	3.696	0.252	0.237	0.01
Minimum			1.118	0.082	0.109	0.151	0.944	0.112	0.005	-0.103
Maksimum			6.707	1.522	0.622	1.476	5.710	0.784	1.722	0.363
Mean			3.061	0.586	0.367	0.576	3.249	0.434	0.575	0.014
St. Dev.			1.82	0.41	0.15	0.36	1.39	0.21	0.52	0.12

Note: < below detection limit

Chloro-Alkaline Indices (CAI) were used to determine the degree of ion exchange reactions between groundwater and aquifer minerals (Schoeller, 1977) . The value of CAI was determined through Equations 2 and 3.

$$CAI - I = \frac{Cl^{-}(Na^{+}+K^{+})}{Cl^{-}} \quad \text{.....(2)}$$

$$CAI - II = \frac{Cl^{-}(Na^{+}+K^{+})}{HCO_3^{-}+SO_4^{2-}+CO_3^{2-}+NO_3^{-}} \quad \text{.....(3)}$$

The CAI index would be positive if there were Na^+ and K^+ ions exchanged by Mg^{2+} and Ca^{2+}. Positive value of CAI indicated a direct reaction of alkaline exchange, or Chloro-Alkali Equilibrium. The negative CAI index showed the exchange reaction in reverse order and was in indirect process. This condition was called Chloro-Alkali Disequilibrium (Hwang *et al*., 2017; Tiwari *et al*., 2020).

Laboratory tests were also using Corrosivity Ratio (CR) that could be used to identify groundwater susceptibility to corrosion.

$$CR = \frac{0.028Cl^{-}+0.021SO_4^{2-}}{[0.02(HCO_3^{-}+CO_3^{2-})]} \quad \text{.....(4)}$$

CR was needed in this study, because groundwater was widely used for distribution to houses. CR will ensure that the water is safe enough if it passes through metal pipes. Determination of CR values used ion Cl^-, SO_4^{2-}, HCO_3^-, and CO_3^{2-}. CR values could be calculated using Equation 2 in mg/l units for each parameter (Kouser *et al.*, 2022).

The research also analyzed the suitability of groundwater if it was used as agricultural irrigation purpose. The used parameters included Sodium Adsorption Ratio (SAR), Soluble Sodium Percentage (SSP), Residual Sodium Carbonate (RSC), Permeable Index (PI), Magnesium Hazard (MH) (Hwang *et al*., 2017; Kouser *et al*., 2022; Tiwari *et al*., 2020).

SAR was used to analyze water for agricultural purposes. SAR was a relative measure of sodium to calcium and magnesium in groundwater (Hwang *et al*., 2017; Sridharan and Senthil Nathan, 2017). SAR values were classified into Excellent (0-10), Good (10-18), Permissible (18 -26), Doubtful/Poor (>26), based on Equation 5.

$$SAR = \frac{Na^{+}}{\sqrt{[(Ca^{2+}+Mg^{2+})/2]}} \quad \text{.....(5)}$$

Soluble Sodium Percentage (SSP) was related to the percentage of Na^+ that could react with the soil. Na^+ exceeding 60 % would degrade the physical farmland condition, so it was not suitable if it was used for agricultural irrigation purpose (Eyankware *et al*., 2020; Li *et al*., 2015). The SSP in groundwater could be known using Equation 6.

$$SSP = \left[\frac{(Na^{+}+K^{+})}{(Ca^{2+}+Mg^{2+}+Na^{+}+K^{+})}\right] X100 \quad \text{.....(6)}$$

SRC was more concerned with levels of CO_3^{2-} and HCO_3^- to Ca^{2+} and Mg^{2+} in groundwater. A high RSC value would damage the soil property (Sridharan and Senthil Nathan, 2017). SRC was divided into three classes which are Good (<1.25), Medium (1.25 – 2.5), and Unsuitable/Bad (>2.5). A high SRC indicated that groundwater could not be used for irrigation (Hwang *et al.*, 2017). Determination of the SRC value used Equation 7.

$$SRC = (HCO_3^{-} + CO_3^{2-}) - (Ca^{2+} + Mg^{2+}) \quad \text{.....(7)}$$

Permeability Index (PI) related to the suitability of groundwater for irrigation based on HCO_3^-, Ca^{2+}, Mg^{2+} and Na^+ in the long-term used (Eyankware *et al*., 2020). PI used the Equation 8.

$$PI = \frac{Na^{+}+\sqrt{HCO_3^{-}}}{Ca^{2+}+Mg^{2+}Na^{+}} \quad \text{.....(8)}$$

PI value was classified into three classifications. Class I is Excellent (PI>75%), Class II is Good (25 % <PI<75 %), and Class III is Unsuitable (PI<25 %).

Magnesium Hazard (MH) indicated the impact of magnesium to groundwater if it was used for irrigation. Equation 9 was used to determine the value of MH.

$$MH = \left(\frac{Mg^{2+}}{(Mg^{2+}+Ca^{2+})}\right) 100\% \quad \text{.....(9)}$$

MH was classified into Suitable (<50 %) and Unsuitable (>50 %). Mg^{2+} levels in groundwater would have an impact in increasing soil alkalinity. These conditions could reduce agricultural yields (Hwang *et al*., 2017).

Result and Analysis

Groundwater Quality

Groundwater samples were taken from traditional shallow dug wells owned by residents. The residents' wells have the average depth of less than 15 m. Table 2 shows the type, colour, EC, DO, and turbidity values of groundwater samples. Most of the groundwater colour was clear, but for Sample 10, the groundwater colour was brownish turbid. The smallest EC value was 132 µS/cm for Sample 4, and the highest one was for Sample 9. All samples had EC values below 1000 µ/cm, indicating very weakly mineralized water (Detay and Carpenter, 1997). Low EC values occurred due to low water-rock interaction, both in the form of mineral dissolution process and evaporation rates (Xu and Su, 2019).

The interaction between rocks and groundwater could also be known by the salinity of groundwater (Table 2). The entire samples had low salinity, so it is categorized as fresh water. Granitic igneous rocks contribute to low mineral concentrations, thus reducing water salinity. Salinity will also increase if the aquifer contains clay (Salami and Akperi, 2023). Sampling locations far from the sea also minimize the interaction of seawater and groundwater. In general, the Na^+, Cl^- concentration, and EC will increase if groundwater is located close to seawater (Hussien and Faiyad, 2016).

The water turbidity indicated the presence of material that scatters a certain amount of light in the water (Jankowski, 2000). A low turbidity value indicated that the water was clear. Sample 6 was the lowest turbidity value, while Sample 10 was the highest turbidity of 331 NTU. Based on Indonesian Government Regulations, the safe turbidity value for drinking water is less than 5 NTU. The study showed that only 6 samples had the turbidity below the maximum allowable limit.

Table 1 and Figure 4 present the concentration of major ions in the Penguluran Basin. The concentration of Ca^{2+} had a range between 1.12 – 6.71 meq/l. Sample 5 had the highest concentration of Ca^{2+}, while Sample 4 had the lowest one. The concentration of Mg^{2+} had the range of 0.08 - 1.52 meq/l, with the highest level was for Sample 5, while the lowest one was for Sample 2. The lowest Na^+ concentration was <0.012 meq/l for Samples 4 and 6, while Na^+ was the highest one for Sample 9. The lowest K^+ concentration was <0.112 meq/l, while the highest one was 1.476 meq/l for Sample 10. HCO_3^- concentration had the lowest value of 0.944 meq/l for Sample 1 and the highest one was 5.710 meq/l for Sample 5. The range of Cl^- concentration was from 0.112 up to 0.784 meq/l. The lowest Cl^- concentration was Sample 2, while highest one was Sample 9. The concentration of SO_4^{2-} was in the range of 0.005 - 1.722 meq/l. The lowest SO_4^{2-} concentration was Sample 2, while highest one was Sample 5.

Figure 5 shows the flownet map of the researched area. The flownet map includes groundwater elevation information, displayed as

Table 2. Type, Colour, EC, pH, DO, and Turbidity Values of Samples

ID Samples	Location	Type	Color	EC (µS/cm)	Salinity (%)	Turbidity (NTU)
1	Ringinkembar	Well	Clear	299	0.01	118
2	Tegalrejo	Well	Clear	190	0	219
3	Sekarbanyu	Well	Clear	248	0	221
4	Argotirto	Well	Clear	132	0	191
5	Harjokuncaran 1	Well	Clear	464	0.01	6
6	Harjokuncaran 2	Well	Clear	214	0	1
7	Sumberagung	Well	Clear	433	0.01	11
8	Sitiarjo 1	Well	Clear	345	0.01	7
9	Sitiarjo 2	Well	Clear	562	0.02	160
10	Sitiarjo 3	Well	Turbid	239	0	331
11	Kedungbanteng 1	Well	Clear	198	0	8
12	Kedungbanteng 2	Well	Clear	262	0.01	148

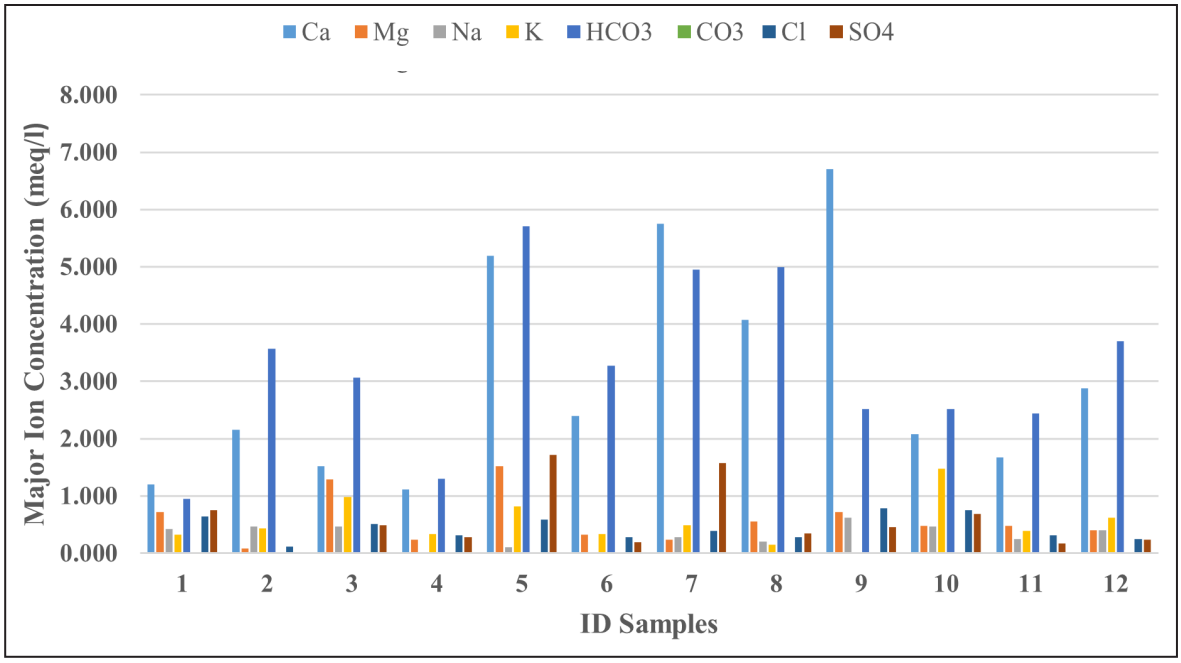

Figure 4. Major ion concentration plotting graph.

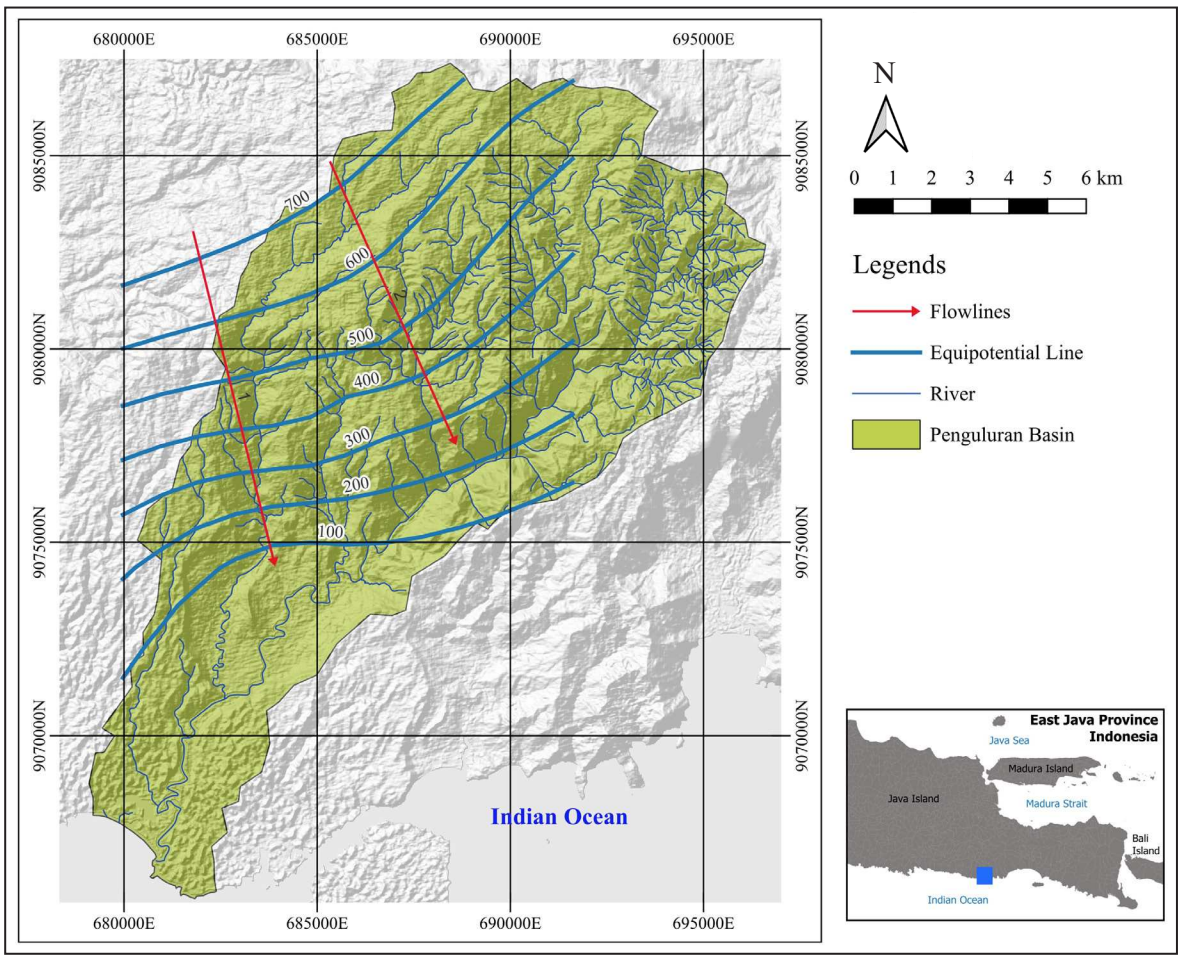

Figure 5. Flownet map.

equipotential lines. Equipotential lines consider the depth of the well water level and its topography (Korkmaz, 2017). Flownets also provide flowline information, which indicates the direction of groundwater flow. The flowlines provide information on both the source and flow direction. A previous research has shown that flowlines can also be used to analyze the source and direction of groundwater pollution, heat transfer, and groundwater well vulnerability (Tóth *et al*., 2023). Based on Figure 4, the groundwater flow direction is towards the southeast, which has a lower topographical contour.

Hydrogeochemical Facies

Hydrogeochemical Facies could be determined by the value of major ions (León *et al*., 2017; Ruiz-Pico *et al.*, 2019). Table 3 shows the hydrogeochemical facies type of groundwater in the studied area. Dissolved cations included K^+, Na^+, Mg^{2+}, Ca^{2+}. Such cations would contribute alkalinity properties into groundwater compared to bicarbonate and carbonate (Jankowski, 2000). Anions included CO^{3-}, HCO_3^-, SO_4^{2-}, Cl^-. The ions composition of groundwater naturally occurred because of the dissolution process in the groundwater (Dogramaci *et al*., 2017).

Hydrogeochemical facies were known through the Piper Trilinear Diagram (Hussien and Faiyad, 2016; Ruiz-Pico *et al*., 2019; Wilopo *et al*., 2020). Piper Trilinear Diagrams were built using diagram software (Figure 6). Overall, hydrogeochemical facies included Ca-Mg-HCO_3 for groundwater samples, except for Sample 1 in the studied site (Table 3). Sample 1 was mixed type which had the same formation with Sample 2 in The Nampol Formation. However, Sample 2 was Ca-Mg-HCO_3 type. The HCO_3^- value for Sample 2 was higher than Sample 1. Nampol Formation contains calcareous sandstone (Sukadana and Indrastomo, 2011). The dissolving process of calcareous sandstone increased the level of HCO_3^- in groundwater (Jankowski, 2000). The high Ca-Mg-HCO_3 was formed due to the presence of bedded reef limestone with varying karstification in the studied area

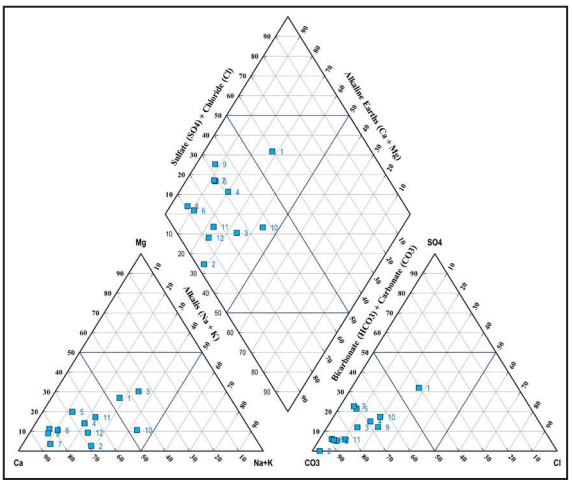

Figure 6. Piper trilinear diagram.

Table 3. Hydrogeochemical Facies

ID	Location	Hydrogeochemical Facies	Kation Type	Anion Type
1	Ringinkembar	Mixed type	No Dominant Type	No Dominant Type
2	Tegalrejo	Ca^{2+}-Mg^{2+}-HCO_3^-	Calcium Type	Bicarbonate Type
3	Sekarbanyu	Mixed type	No Dominant Type	Bicarbonate Type
4	Argotirto	Ca^{2+}-Mg^{2+}-HCO_3^-	Calcium Type	Bicarbonate Type
5	Harjokuncaran 1	Ca^{2+}-Mg^{2+}-HCO_3^-	Calcium Type	Bicarbonate Type
6	Harjokuncaran 2	Ca^{2+}-Mg^{2+}-HCO_3^-	Calcium Type	Bicarbonate Type
7	Sumberagung	Ca^{2+}-Mg^{2+}-HCO_3^-	Calcium Type	Bicarbonate Type
8	Sitiarjo 1	Ca^{2+}-Mg^{2+}-HCO_3^-	Calcium Type	Bicarbonate Type
9	Sitiarjo 2	Ca^{2+}-Mg^{2+}-HCO_3^-	Calcium Type	Bicarbonate Type
10	Sitiarjo 3	Mixed type	No Dominant Type	Bicarbonate Type
11	Kedungbanteng 1	Ca^{2+}-Mg^{2+}-HCO_3^-	Calcium Type	Bicarbonate Type
12	Kedungbanteng 2	Ca^{2+}-Mg^{2+}-HCO_3^-	Calcium Type	Bicarbonate Type

(Poespowardoyo, 1975). High concentrations of Ca-Mg-HCO_3 can also occur in volcanic rocks, as shown in studies following the La Palma volcanic eruption and in the Malabar Tilu deposits (Jiménez *et al.*, 2024; Maria *et al.*, 2021). Enrichment of Ca^{2+}-Mg^{2+} typically occurs in shallow groundwater (Maria *et al.*, 2021; Salami and Akperi, 2023). The process of water acidification due to interaction with rocks containing Ca^{2+}-Mg^{2+} will also increase the levels of Ca^{2+}-Mg^{2+} in groundwater (Jiménez-Valera *et al.*, 2023). A previous research states that Ca^{2+} weathering in silica-rich minerals originating from basaltic andesitic volcanic rocks will also increase Ca^{2+} (Maria *et al.*, 2021). Shallow groundwater in Merapi Volcano also has groundwater rich in Ca^{2+}-Mg^{2+} (Hendrayana *et al.*, 2023). This aligns with the conditions of the studied area, which is dominated by andesitic rocks, basaltic lava, and tuff (Bemmelen, 1949), as well as in its shallow groundwater.

Figure 7 shows the orders of cations (Figure 7a) and anions (Figure 7b) in the groundwater of Penguluran Basin. The figure shows that Ca^{2+} is the dominant cation, while HCO_3^- is the dominant anion. The cation concentration was $Ca^{2+} > Mg^{2+} > Na^{+} > K$, while the anion was $HCO_3^- > Cl^- > SO_4^{2-}$.

Cation levels are shown as Ca-Mg-(Na+K) in the cation triangle, where about 75 % of the samples were dominated by the calcium type. The remaining percentage of those samples belonged to the no dominant type, specifically Samples 1, 3, and 10. Samples 1 and 3 were located in The Nampol Formation (Tmn), and Sample 10 was in The Wonosari Formation (Tmwl). The highest Ca concentration was 6,707 meq/l for Sample 9, while the lowest was 1,118 meq/l for Sample 4. Sample 9 was found in the limestone formation. Sample 4 was in the tuff member of The Mandalika Formation (Tomt), which consists of tuff breccia sediment with low calcium levels. The highest sodium in The Penguluran Basin of 0.622 meq/l was for Sample 9 in Tmwl Formation. The lowest sodium was for Sample 4 in Tomt Formation. The highest potassium value of 1,476 meq/l was for Sample 10 in the Tmwl Formation. The lowest potassium value was for Sample 9 in the Tuff Formation. Based on the cation triangle, the groundwater is classified as alkaline water,

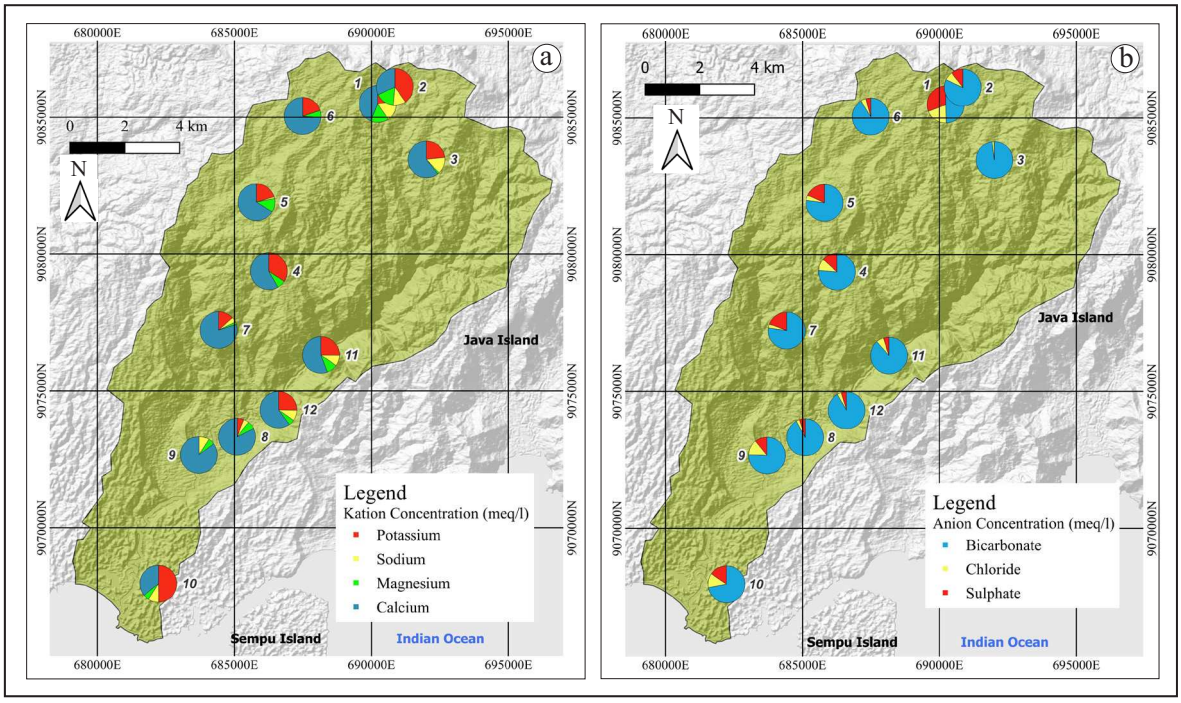

Figure 7. (a). Cation and (b). anion in groundwater of Penguluran Basin.

characterized by high $Na^{+}+K^{+}$ and low calcium content, along with low water hardness (Hwang *et al*., 2017).

Anion levels are shown by HCO_3^- Cl-SO_4 in the anion triangle. In the anion triangle, 91 % of groundwater samples were dominated by bicarbonate type, and 9 % were no dominant type. HCO_3^- in groundwater would impact to groundwater to be alkaline. This condition is consistent with the cation triangle tendency towards alkalinity. Alkalinity in natural groundwater was produced by the dissolution of carbon dioxide, bicarbonate, and carbonate (Jankowski, 2000). Alkaline groundwater could be formed by fractions of CO_2 gas in the atmosphere, atmospheric gases in the soil, and groundwater. Other sources could come from sulphate reduction and carbonate rock metamorphism (Weight, 2008), microbial respiration (Eslami *et al*., 2019), and silica weathering in clays that released carbonate and bicarbonate ions (Ruiz-Pico *et al*., 2019). The lowest alkalinity in bicarbonate form of 0.944 meq/l was for Sample 1, while the highest one of 5,710 meq/l was for Sample 5 in Nampol Formation. High HCO_3^- indicated that groundwater was rich in dissolved CO_2 (Yan *et al*., 2021). The value of chloride in groundwater was generally lower than in other major constituents. Sample 9 had the highest chloride value of 0.784 meq/l, which was in Wonosari Formation. Sample 2 had the lowest chloride content of 0.112 meq/l, which was in Nampol Formation consisting of tuffaceous sandstone. The highest sulphate of 1,722 meq/l was for Sample 5, while the lowest sulphate of 0.005 meq/l was for Sample 2. Samples 5 and 2 were in Nampol Formation. However, Sample 5 is located closer to Mandalika Formation, which consists of andesitic-basaltic rocks (Heru and Prasetia, 2024).

Weathering Types

Naturally, groundwater quality results from the interaction between chemical elements in rocks and groundwater. One method to identify this process is through analysis using a Gibbs Diagram. Figure 8 presents the Gibbs Diagram, which is utilized to identify the processes controlling the hydrogeochemistry of groundwater. The diagram also provides information on Total Dissolved Solids (TDS), which represents the amount of dissolved solids in groundwater (Gao *et al*., 2020). All groundwater samples had a TDS value between 142.60 and 608.90 mg/l. The Gibbs Diagram further shows that all groundwater samples fall within the weathering dominance group. This indicates that the groundwater chemistry is primarily influenced by rock weathering processes (rock dominance) (Razi *et al*., 2024).

Figure 9 is a weathering scatter diagram of rocks with a 1:1 dash line in scale (Kaur *et*

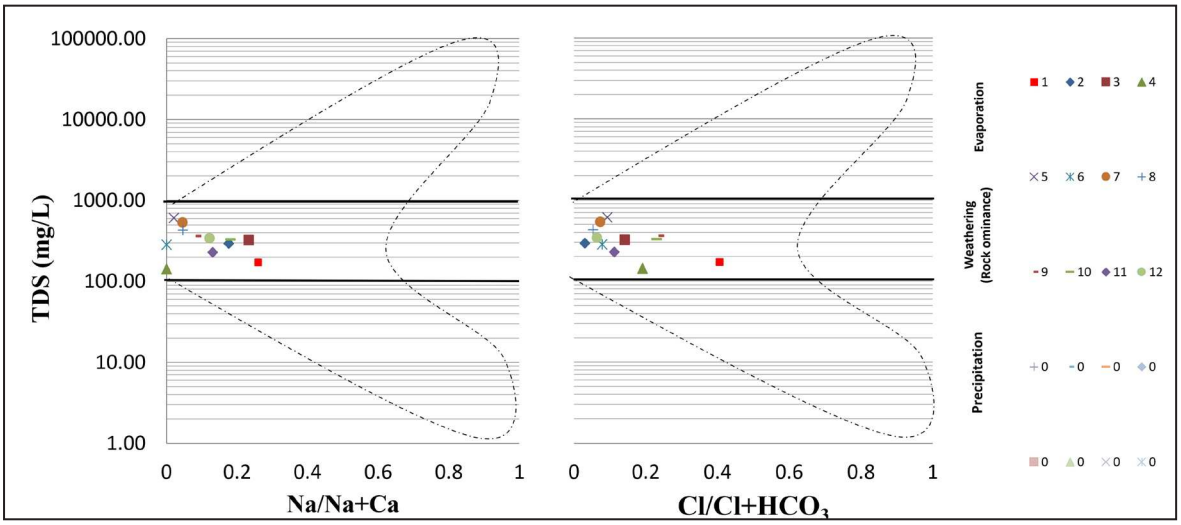

Figure 8. Gibbs diagram.

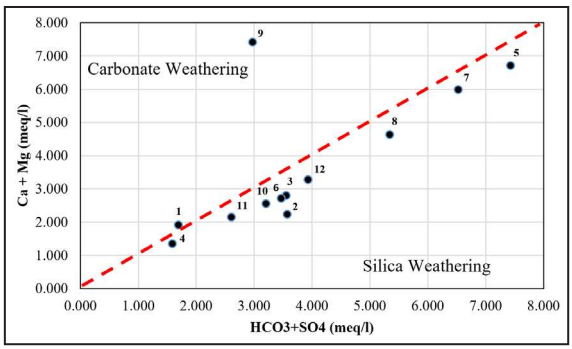

Figure 9. Plot of HCO_3+SO4 vs Ca+Mg^{2+} (Modified from (Kaur *et al.*, 2017).

al., 2017). This diagram is used to analyze the weathering process through the identification of HCO_3^-+SO_4^{2-} versus Ca^{2+}+Mg^{2+} concentrations. The graph in Figure 9 shows two weathering groups: carbonate weathering (above the red line) and silica weathering (below the red line). Groundwater samples falling into the carbonate weathering group are Samples 1 and 9. Sample 1 is located in The Wuni Formation, which consists of basaltic, andesitic, and tuff rocks. However, Sample 1 is situated close to the red boundary line. Sample 1 is also adjacent to Sample 4, which was collected from the tuff member of Mandalika Formation. Both of these samples show relatively low ion concentrations. Low ion concentrations can occur in areas with less intensive weathering or shorter water-rock contact times. Sample 9 is located in Wonosari Formation (Tmwl), which consists of limestone, calcareous sandstone, sandy marl, and claystone intercalations (Juwono *et al*., 2022). This indicates that the groundwater is intensively dissolving calcium carbonate and magnesium carbonate minerals.

Most of the groundwater samples fall within the silica weathering process. Samples belonging to this group include: 2, 3, 4, 5, 6, 7, 8, 10, 11, and 12. The high number of samples categorized under silica weathering aligns with the geological conditions in the studied area, which are dominated by old volcanic rock deposits and volcaniclastic sedimentary rocks (Bemmelen, 1949). These rocks include andesite, basaltic, trachyitic, and dacitic lava, as well as propylitized andesitic breccia (Yuwanto and Ridwan, 2017; Heru and Prasetia, 2024), clastic sedimentary material and tuffaceous sandstone (Sukadana and Indrastomo, 2011). Mandalika Formation is the most widespread formation in the studied area. The formation contains silica varying from moderate to high (Heru and Prasetia, 2024). This sufficient content proves the dominant silica weathering process in the studied area.

Chloro-Alkaline Indices (CAI)

Chloro-Alkaline Indices (CAI) I-II were calculated using Equations 2 and 3 (Schoeller, 1977). The calculation of CAI-I and II resulted that 83 % had negative values. Most samples reflected the same cation exchange (Figure 10). This study is similar to the research by Yan *et al.* (2021) which also had negative CAI-I and CAI-II values in the areas consisted of dolomite, gypsum, and calcite rocks. A negative CAI value described that there was an exchange of Ca^{2+} and Mg^{2+} ions from water with Na^+ and K^+ from rocks. CAI-I values was from -5,902 to -0.220. CAI-II had range values of -0.221 to -0.002. Such conditions would increase Ca and Mg in groundwater (Yan *et al*., 2021).

CAI-I and CAI-II were positive for about 17 % of the total sample. A positive CAI value illustrates that there was a directly exchange of Na^+ and K^+ ions from water with Ca^{2+} and Mg^{2+} from rocks (Singh *et al*., 2020). CAI-I had range of 0.026 and 0.486, while CAI-II was between 0.005 and 0.069. Samples 1 and 9 had CAI-I and

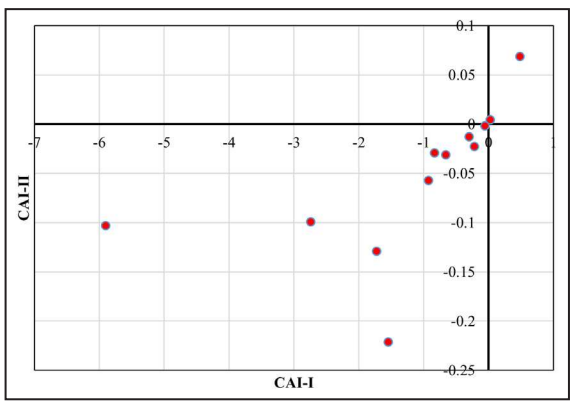

Figure 10. CAI-I vs CAI-II.

CAI-II in positive values. Sample 9 had a lower K^+ value and was dominated by Na^+. About 83 % of the samples showed silicate weathering, and had negative CAI-I and CAI-II values. A CAI value dominated by negative values indicated that the cation exchange determined the chemical composition of groundwater (Hartanto and Lubis, 2023; Singh *et al*., 2020).

Corosivity Ratio

Corrosivity Ratio (CR) is a vulnerability level indicator of groundwater to the corrosion risk (Rout and Setia, 2018). Groundwater is used for various purposes. In water distribution systems for water supply, water with corrosive properties will easily damage pipes, especially metallic pipes, leading to leaks (Siddha and Sahu, 2022). A CR of <1 indicated that the groundwater was safe, while if it was >1, the groundwater was corrosive (Kaur *et al*., 2017). The CR value was calculated using Equation 2. About 92 % groundwater in the studied area was corrosive-safe, while that remaining was unsafe. The CR value indicated corrosive-safe groundwater was between 0.027 and 0.469 (Figure 11).

Hydrogeochemical facies in groundwater showed that all samples belonged to the bicarbonate anion type with low CR values. Based on Piper Trilinear Diagram, only Sample 1 was the non-dominant type which had unsafe CR value of 1,209. This indicates that for Sample 1, the groundwater is unsafe for piping networks that use metallic pipes (Hwang *et al*., 2017; Siddha and Sahu, 2022).

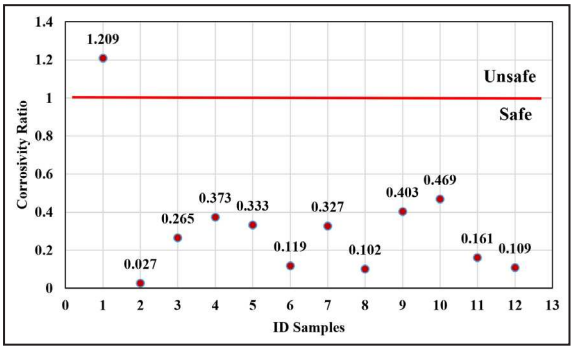

Figure 11. Corrosivity ratio on each groundwater samples.

Groundwater Suitability for Irrigation Purposes

The identifications of groundwater suitability for agriculture in this study were SAR, SSP, RSC, PI, and MH. The five indices show the interaction between groundwater and soil. Such interactions could have an impact on soil and plants. SAR, SSP, and RSC considered Na^+ in groundwater. High Na^+ and Mg^{2+} in groundwater would harm soil property.

Sodium Absorption Ratio (SAR)

SAR is a relative measure of sodium to calcium and magnesium in groundwater (Hwang *et al*., 2017; Sridharan and Senthil Nathan, 2017). SAR showed alkalinity hazard on groundwater, which could interfere to plant growth (Jalil *et al*., 2020). The SAR value was calculated based on Equation 5. The calculation results indicated that 50 % were the Poor class, 33 % were Good, and 17 % were Excellent if groundwater was used for agriculture (Table 4). Areas which had poor class of SAR values were located in the northern and southern sides of the basin. Figure 12 is a SAR vs EC data plot using US Salinity Laboratory (USSL) Diagram. The classification results showed that 25 % of the samples were C1S1, 50 % were C1S2, and 25 % were C1S3. Overall, the sample had low Na^+ levels with varying salinity. In C1S3, groundwater conditions were salty, with low Na+, but it could be used with certain treatments.

Soluble Sodium Percentage (SSP)

SSP (% Na) was also used to determine the groundwater suitability in agricultural irrigation purposes. SSP is a sodium hazard as percentage of Na^+ to other ions. If the SSP > 60 % resulted soil aggregate dispersion, it would harm to plants and soil (Jalil *et al*., 2020). SSP classification was based on Equation 6. The result of SSP Classification were 33 % Excellent, 42 % were Good, and 25 % were Fair (Table 4). Classification of SSPs on Wilcox Diagrams through SSP and EC plots used DIAGRAMMES software (Figure12b). The SSP vs EC plot results in Figure 12, show that

Table 4. Groundwater Classifications by SAR, SSP, RSC, PI, MH

Indicator	Value	Suitability	% Samples	Number of samples
SAR	0–10	Excellent	16.6	2
	10–18	Good	33.3	4
	18–26	Permissible	-	0
	>26	Poor/Doubtful	50	6
SSP (% Na)	<20	Excellent	33	4
	20–40	Good	42	5
	40–80	Fair	25	3
	>80	Poor	-	0
RSC	<1.25	Safe/Good	92	11
	1.25–2.5	Medium/Marginal	8	1
	>2.5	Unsuitable	-	0
PI	>75%	Excellent	-	0
	25–75%	Good	83	10
	<25%	Unsuitable	17	2
MH	<50%	Suitable	100	12
	>50	Unsuitable	-	0

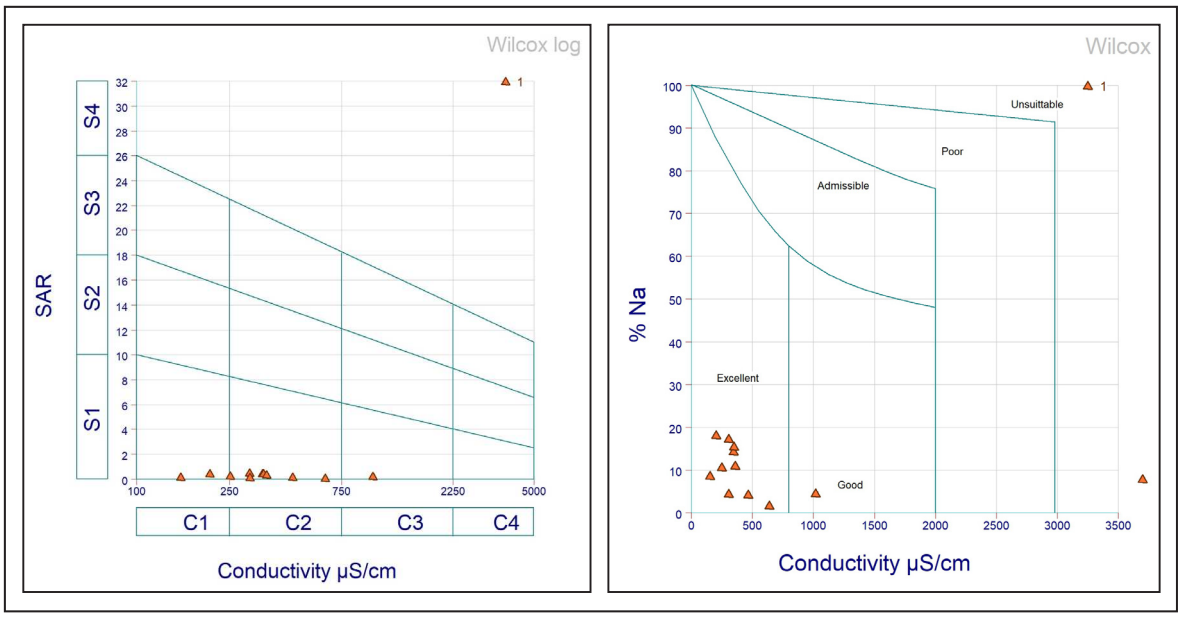

Figure 12. SAR and SSP (% Na).

most groundwater samples were in Excellent and Good classes. This indicated that the most samples were in safe condition if they were used for agricultural irrigation purposes.

Residual Sodium Carbonate (RSC)

RSC indicated bicarbonate hazard to groundwater (Jalil *et al*., 2020). RSC considered bicarbonate and carbonate levels against calcium and magnesium. Identification of the RSC was important, because the studied area contains limestone located near its surface. RSC determination used Equation 7, and was classified using Table 4. The calculation results showed that 45 % of the samples had negative RSC values. The value indicated that the amount of calcium and magnesium were greater than carbonate and bicarbonate. The RSC values in the studied area were classified into 92 % (safe/good) and 8 % medium/marginal. Based on the class of RSC, generally groundwater was quite safe for irrigation purposes.

Permeability Index (PI)

PI indicated the effect of groundwater to soil permeability. PI was calculated based on exposure to sodium, calcium, magnesium, and bicarbonate in groundwater (Eyankware *et al*., 2020). A high PI value indicated good permeability, so it could supply groundwater, but it was also susceptible to pollution (Mansouri *et al*., 2022). Table 4 shows the PI values were classified into 83 % Good, and 17 % Unsuitable. The unsuitable PI were for Samples 5 and 7.

Magnesium Hazard (MH)

Mg^{2+} levels increased if they occurred due to Na in irrigated soils. Increased magnesium in the soil caused soil sodication, which ruined the clay structure. In these conditions, the relative value of hydraulic conductivity would decrease, because Mg^{2+} in the soil behaved like Na^{+} (Hwang *et al.*, 2017). If the MH value in groundwater was <50 %, then groundwater was safe to be used for agriculture purposes (Jalil *et al*., 2020). Overall groundwater samples in the basin had a low MH, so they were suitable for irrigation (Table 4).

Anthropogenic Impact

Hydrogeochemical conditions of aquifers were also influenced by human activity (Appelo and Postma, 1993; Hussein *et al*., 2019; Sun and Liu, 2023). Shallow aquifer had high susceptibility of anthropogenic activity (Ekere *et al*., 2019). The anthropogenic impact on groundwater could be observed through EC and potassium concentration (Ruiz-Pico *et al*., 2019). If EC and potassium levels were low, the anthropological impact on groundwater was also in small intensity. Ca^{2+}+ Mg^{2+} vs SO_4 + HCO_3^- concentrations could also be used to determine the anthropogenic impact on groundwater (Yan *et al*., 2021). Figure 13 shows that the slope of the linear fitting equation for Ca^{2+}+Mg^{2+} vs SO_4^{2-} + HCO_3^- is R^2 = 0.4869. This value indicates that the alkaline nature of the groundwater is closely related to natural weathering.

Groundwater samples related to anthropogenic impact are Samples 1 and 9. Considering the hydrogeochemical processes, Sample 1 falls into the mixed type category. In Figure 13, Sample 1 is close to the 1:1 line. Thus, Sample 1 shows the presence of anthropogenic impact factors, but still retains cation exchange properties. It is different from Sample 9, which falls into the anthropogenic impact category based on the Ca^{2+}+Mg^{2+} vs SO_4^{2-} + HCO_3^- concentrations, and deviates significantly from the 1:1 line. Figure 13 also shows samples belonging to the cation exchange group, namely samples 2, 3, 4, 5, 6, 7, 8, 10, 11, and 12. However, overall, the samples belonging to the cation exchange group are close to the 1:1 line. This indicates a continuing possibility of anthropogenic impact influencing the concentrations of Ca^{2+}+Mg^{2+} and SO_4^{2-} + HCO_3^-.

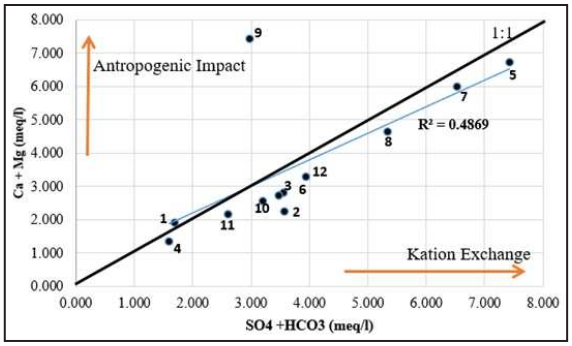

Figure 13. Ca^{2+}+ Mg vs SO4 + HCO3 (Modified from (Yan *et al*., 2021)).

Other studies mentioned that using nitrate was more depicted as the anthropogenic impact to groundwater (Re *et al*., 2017; Adimalla *et al*., 2021; Li *et al*., 2021). Natural groundwater did not form nitrates in the water. Nitrate levels in groundwater were more influenced by factors such as geography, landuse, hydrological characteristics, and climate (Li *et al*., 2021; Xie *et al*., 2021). Indonesian Government Regulations provided guidelines that the maximum level of nitrates in the water was 10 mg/l. Figure 14 shows the nitrate levels when they are compared to government guidelines. The study resulted that 17 % of the samples were below the maximum allowable limit. About 25 % of the samples were close to the level, while the remaining of 58 % exceeded the government allowable limit.

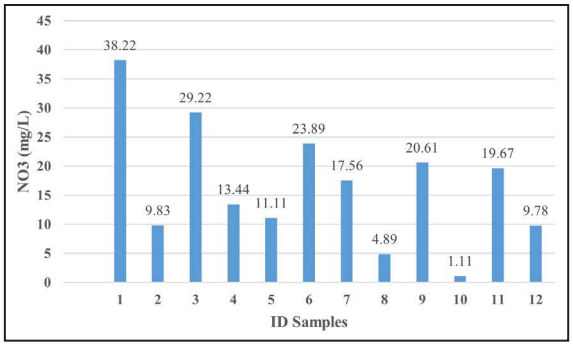

Figure 14. Nitrate concentration in each groundwater sample.

Settlements were randomly located and varied with other landuse such as forests, mixed gardens, and farms. Nitrate would increase if there was agricultural activity, and it causes agricultural pollution (Re *et al*., 2017; Li *et al*., 2021). The location of wells which were close to human activities and animal husbandry area would also increase the nitrate levels (Li *et al.*, 2021). Groundwater pollution caused by nitrate (groundwater nitrate pollution) would be aggravated if the people population had poor sanitation (Bu *et al*., 2020; Adimalla *et al.*, 2021). If it was associated with a maximum limit of nitrate concentration in groundwater which was 10 mg/l, then the groundwater in the Penguluran Basin had been polluted due to anthropogenic activity (Yan *et al*., 2021).

Conclusions

This study successfully characterized the hydrogeochemical features and assessed the groundwater quality of the shallow aquifer system in the Penguluran Basin, East Java, Indonesia. The groundwater is predominantly of the Ca-Mg-HCO_3 hydrogeochemical facies, dominated by Ca^{2+} cations and HCO_3^- anions. Most samples indicate freshwater characteristics formed by silicate weathering, exhibiting low corrosivity risk. Furthermore, the groundwater quality generally falls within good to excellent classes for irrigation purposes. However, anthropogenic impacts were evident, with more than half of the samples exceeding safe nitrate concentrations, highlighting a significant threat to groundwater sustainability.

The study accomplished its goals by inventorying groundwater resources, analyzing important hydrochemical processes, determining the water suitability for irrigation, and identifying probable anthropogenic contamination sources. Despite this accomplishment, the study is restricted by the small number of sampling locations and the lack of temporal (seasonal) monitoring, which may impair the robustness of groundwater quality assessments over time.

Future research should include expanding sampling coverage both spatially and seasonally, using stable isotope techniques to better trace pollutant origins, and incorporating numerical hydrogeological modelling to predict groundwater quality changes under increasing anthropogenic pressures and climate variability. These developments are critical for developing sustainable groundwater management techniques in karstic and sedimentary aquifer systems.

Acknowledgments

The first author would like to thank the Universitas Negeri Malang through research funding. The author would also like to thank the laboratory assistants for helping in sample collection and laboratory analysis. A word of gratitude is also extended to anonymous reviewers for their very valuable suggestions.

References

Adimalla, N., Qian, H., and Tiwari, D.M., 2021. Groundwater chemistry, distribution and potential health risk appraisal of nitrate enriched groundwater: A case study from the semi-urban region of South India. *Ecotoxicology and Environmental Safety*, 207. DOI:10.1016/j.ecoenv.2020.111277.

Ahirwar, S., Malik, M.S., Ahirwar, R., and Shukla, J.P., 2020. Identification of suitable sites and structures for artificial groundwater recharge for sustainable groundwater resource

development and management. *Groundwater for Sustainable Development*, *11* (February), 100388. DOI:10.1016/j.gsd.2020.100388.

Appelo, C.A.J. and Postma, D., 1993. Geochemistry, groundwater and pollution. *Geochemistry, Groundwater and Pollution*. DOI:10.1016/0016-7037(94)90585-1.

Arifianto, A.K., 2016. Analisis Pengembangan Air Bawah Tanah Terhadap Kepuasan Masyarakat di Kecamatan Sumbermanjing Wetan Kabupaten Malang. *Jurnal Reka Buana,* 2 (1), p.30-46. http://fisikaituasyik.weebly.com/debit-

Asadi, E., Isazadeh, M., Samadianfard, S., Ramli, M.F., Mosavi, A., Nabipour, N., Shamshirband, S., Hajnal, E., and Chau, K.W., 2020. Groundwater quality assessment for sustainable drinking and irrigation. *Sustainability (Switzerland)*, 12 (1), 13pp. DOI:10.3390/su12010177.

Bemmelen, R. Van, 1949. *The Geology of Indonesia Vol. IA* (General Geology of Indonesia and Adjacent Archipelagoes). Government Printing Office.

Bouderbala, A., 2020. Groundwater quality assessment of the coastal alluvial aquifer of Wadi Hachem, Tipaza, Algieria. *Environmental and Socio-Economic Studies*, 8 (4), p.11-23. DOI:10.2478/environ-2020-0020.

BPS, 2019. *Statistik Air Bersih Jawa Timur 2019*. Badan Pusat Statistik Provinsi Jawa TImur.

Bremard, T., 2022. Monitoring Land Subsidence: The Challenges of Producing Knowledge and Groundwater Management Indicators in the Bangkok Metropolitan Region, Thailand. *Sustainability (Switzerland)*, 14 (17), 25pp. DOI:10.3390/su141710593.

Bu, J., Sun, Z., Ma, R., Liu, Y., Gong, X., Pan, Z., and Wei, W., 2020. Shallow groundwater quality and its controlling factors in the su-xi-chang region, eastern china. *International Journal of Environmental Research and Public Health*, 17 (4), 18pp. DOI:10.3390/ijerph17041267.

Detay, M. and Carpenter, M., 1997. *Water wells: implementation, main-tenance and restoration*. Wiley .

Dogramaci, S., McLean, L., and Skrzypek, G., 2017. Hydrochemical and stable isotope indicators of pyrite oxidation in carbonate-rich environment; the Hamersley Basin, Western Australia. *Journal of Hydrology*, 545, p.288-298. DOI:10.1016/ j.jhydrol.2016.12.009.

Egbueri, J.C., Ezugwu, C.K., Unigwe, C.O., Onwuka, O.S., Onyemesili, O.C., and Mgbenu, C.N., 2021. Multidimensional Analysis of the Contamination Status, Corrosivity and Hydrogeochemistry of Groundwater from Parts of the Anambra Basin, Nigeria. *Analytical Letters*, 54 (13), p.2126-2156. DOI:10.1080/00032719.2020.1843049

Ekere, N.R., Agbazue, V.E., Ngang, B.U., and Ihedioha, J.N., 2019. Hydrochemistry and Water Quality Index of groundwater resources in Enugu north district, Enugu, Nigeria. *Environmental Monitoring and Assessment*, 191 (3), p.1-15. DOI:10.1007/s10661-019-7271-0.

Eslami, F., Yaghmaeian, K., Mohammadi, A., Salari, M., and Faraji, M., 2019. An integrated evaluation of groundwater quality using drinking water quality indices and hydrochemical characteristics: a case study in Jiroft, Iran. *Environmental Earth Sciences*, 78 (10), 10pp. DOI:10.1007/s12665-019-8321-1.

Eyankware, M.O., Aleke, C.G., Selemo, A.O.I., and Nnabo, P.N., 2020. Hydrogeochemical studies and suitability assessment of groundwater quality for irrigation at Warri and environs, Niger delta basin, Nigeria. *Groundwater for Sustainable Development*, *10*. DOI:10.1016/j.gsd.2019.100293.

Gao, Y., Qian, H., Ren, W., Wang, H., Liu, F., and Yang, F., 2020. Hydrogeochemical characterization and quality assessment of groundwater based on integrated-weight water quality index in a concentrated urban area. *Journal of Cleaner Production*, *260*. DOI:10.1016/j.jclepro.2020.121006

Geological Agency of Indonesia, 2010. *Geological Map of Indonesia*.

Ghalib, H.B., 2017. Groundwater chemistry evaluation for drinking and irrigation utilities in east Wasit province, Central Iraq. *Applied Wa-*

ter Science, 7 (7), p.3447-3467. DOI:10.1007/s13201-017-0575-8.

Gibrilla, A., Osae, S., Akiti, T.T., Adomako, D., Ganyaglo, Samuel. Y., Bam, Edward. P.K., and Hadisu, A., 2010. Hydrogeochemical and Groundwater Quality Studies in the Northern Part of the Densu River Basin of Ghana. *Journal of Water Resource and Protection*, 02 (12), p.1071-1081. DOI:10.4236/jwarp.2010.212126.

Gonzales Amaya, A., Ortiz, J., Durán, A., and Villazon, M., 2019. Hydrogeophysical methods and hydrogeological models: basis for groundwater sustainable management in Valle Alto (Bolivia). *Sustainable Water Resources Management*, 5 (3), p.1179-1188. DOI:10.1007/s40899-018-0293-x.

Hartanto, P. and Lubis, R.F., 2023. Use the hot spring's Chloro-Alkaline Index (CAI) for the low enthalpy prospect of the Rawadanau geothermal field. *Journal of Physics: Conference Series*, 2596 (1), 6pp. DOI:10.1088/1742-6596/2596/1/012049.

Hendrayana, H., Harijoko, A., Riyanto, I.A., Nuha, A., and Ruslisan, 2023. Groundwater Chemistry Characterization in The South and Southeast Merapi Volcano, Indonesia. *Indonesian Journal of Geography*, 55 (1), p.10-29. DOI:10.22146/ijg.76433.

Heru, S. and Prasetia, G.E,. 2024. Geologi dan Karakteristik Mineral Piropilit Daerah Sumbermanjing Wetan, Malang. *Jurnal Geosaintek*, 10 (3), p.198-206. DOI:10.12962/j25023659.v10i3.1816.

Hussien, B.M. and Faiyad, A.S., 2016. Modeling the Hydrogeochemical Processes and Source of Ions in the Groundwater of Aquifers within Kasra-Nukhaib Region (West Iraq). *International Journal of Geosciences*, 07 (10), p.1156-1181. DOI:10.4236/ijg.2016.710087.

Hussein, E.E., Fouad, M., and Gad, M.I., 2019. Prediction of the pollutants movements from the polluted industrial zone in 10th of Ramadan city to the Quaternary aquifer. *Applied Water Science*, 9 (1), p.1-19. DOI:10.1007/s13201-019-0897-9.

Hwang, J.Y., Park, S., Kim, H.K., Kim, M.S., Jo, H.J., Kim, J.I., Lee, G.M., Shin, IK., and Kim, T.S., 2017. Hydrochemistry for the Assessment of Groundwater Quality in Korea. *Journal of Agricultural Chemistry and Environment*, 06 (01), p.1-29. DOI:10.4236/jacen.2017.61001.

Jalil, A., Luyun, Jr. R., Delos Reyes, Jr. A., and Bato, V., 2020. Assessment of Groundwater Quality for Irrigation at Malamawi Island, Basilan, Philippinnes. *Jurnal Penelitian Pengelolaan Daerah Aliran Sungai,* 4 (2), p.187-200. DOI:10.20886/jppdas. 2020.4.2.187-200.

Jankowski, J., 2000. *Hydrogeochemistry* . UNSW Groundwater Centre, The University of South New Wales.

Jiménez-Valera, J.A., Alhama, I., and Trigueros, E., 2023. Quantification of Groundwater Vertical Flow from Temperature Profiles: Application to Agua Amarga Coastal Aquifer (SE Spain) Submitted to Artificial Recharge. *Water*, 15 (6), 17pp. DOI:10.3390/w15061093.

Jiménez, J., Gasco Cavero, S., Marazuela, M.Á., Baquedano, C., Laspidou, C., Santamarta, J. C., and García-Gil, A.. 2024. Effects of the 2021 La Palma volcanic eruption on groundwater hydrochemistry: Geochemical modelling of endogenous CO2 release to surface reservoirs, water-rock interaction and influence of thermal and seawater. *Science of the Total Environment*, 929. DOI:10.1016/j.scitotenv.2024.172594.

Juwono, A.M., Susilo, A., Sunaryo, Aprilia, F., and Hisyam, F., 2022. Study of Surface Conditions of Southern Cross Road Using The Wenner-Schlumberger Method for Disaster Mitigation. *International Journal of GEOMATE*, 23 (97), p.97-105. DOI:10.21660/2022.97.3261.

Kaur, T., Bhardwaj, R., and Arora, S., 2017. Assessment of groundwater quality for drinking and irrigation purposes using hydrochemical studies in Malwa region, southwestern part of Punjab, India. *Applied Water Science*, 7 (6), p.3301-3316. DOI:10.1007/s13201-016-0476-2.

Korkmaz, S., 2017. Analytical solutions to groundwater flow around wells using discharge potential. *European Water*, *57*.

Kouser, B., Bala, A., Verma, O., Prashanth, M., Khosla, A., and Pir, R.A., 2022. Hydrochemistry for the assessment of groundwater quality in the Kathua region, Jammu and Kashmir, India. *Applied Water Science*, 12 (7), 22pp. DOI:10.1007/s13201-022-01673-9.

León, G.S. de, Leal, J.A.R., Ramírez, J.M., Álvarez, B.L., and León, E.E.S. de, 2017. Quality Indices of Groundwater for Agricultural Use in the Soconusco, Chiapas, Mexico. *Earth Sciences Research Journal,* 21 (3), p.117-127. DOI:10.15446/esrj.v21n3. 63455.

Li, P., Wu, J., and Qian, H., 2015. Hydrogeochemistry and quality assessment of shallow groundwater in the southern part of the yellow river alluvial plain (Zhongwei section), Northwest China. *Earth Sciences Research Journal*, 18 (1), p. 27-38. DOI:10.15446/esrj.v18n1.34048.

Li, X., Wu, H., Qian, H., and Gao, Y., 2018. Groundwater chemistry regulated by hydrochemical processes and geological structures: A case study in Tongchuan, China. *Water (Switzerland)*, 10, 338. DOI:10.3390/w10030338.

Li, Y., Bi, Y., Mi, W., Xie, S., and Ji, L., 2021. Land-use change caused by anthropogenic activities increase fluoride and arsenic pollution in groundwater and human health risk. *Journal of Hazardous Materials*, 406. DOI:10.1016/j.jhazmat.2020.124337.

Mansouri, Z., Leghrieb, Y., Kouadri, S., Al-Ansari, N., Najm, H.M., Mashaan, N.S., Eldirderi, M.M.A., and Khedher, K.M., 2022. Hydro-Geochemistry and Groundwater Quality Assessment of Ouargla Basin, South of Algeria. *Water (Switzerland)*, 14 (15), 20pp. DOI:10.3390/w14152441.

Marganingrum, D., 2018. Carrying capacity of water resources in Bandung Basin. *IOP Conference Series: Earth and Environmental Science*, 118 (1), 7pp. DOI:10.1088/1755-1315/118/1/012026.

Maria, R., Satrio, Iskandarsyah, T. Y. W. M., Suganda, B. R., Delinom, R. M., Marganingrum, D., Purwoko, W., Sukmayadi, D., and Hendarmawan, H., 2021. Groundwater recharge area based on hydrochemical and environmental isotopes analysis in the south bandung volcanic area. *Indonesian Journal of Chemistry*, 21 (3), p.609-625. DOI:10.22146/ijc.58633.

Mujib, M.A., Adji, T.N., Haryono, E., Naufal, M., and Fatchurohman, H., 2024. Karst Aquifer Characterization by Means of Its Karstification Degree and Time Series Analysis (Case: Ngerong Spring in Rengel Karst, East Java, Indonesia). *Indonesian Journal on Geoscience*, 11 (1), p.45-60. DOI:10.17014/ijog.11.1.45-60.

Poespowardoyo, S., 1975. *Indonesia Hydrogeology Map, Sheet X Kediri, Scale 1:250.000.*

Poetra, R.P., Adji, T.N., Santosa, L.W., and Khakhim, N., 2020-. Hydrogeochemical Conditions in Groundwater Systems with Various Geomorphological Units in Kulonprogo Regency, Java Island, Indonesia. *Aquatic Geochemistry*, 26 (4), p.421-454. DOI:10.1007/s10498-020-09384-w.

Ram, A., Tiwari, S.K., Pandey, H.K., Chaurasia, A.K., and Chaudhary, S.K., 2020. Assessment of Groundwater behavior in Kulpahar Watershed, District Mahoba, Uttar Pradesh, India. *IOP Conference Series: Earth and Environmental Science*, 597 (1), 16pp. DOI:10.1088/1755-1315/597/1/012014.

Razi, M.H., Wilopo, W., and Putra, D.P.E., 2024. Hydrogeochemical evolution and water–rock interaction processes in the multilayer volcanic aquifer of Yogyakarta-Sleman Groundwater Basin, Indonesia. *Environmental Earth Sciences*, 83 (6), 17pp. DOI:10.1007/s12665-024-11477-6.

Re, V., Sacchi, E., Kammoun, S., Tringali, C., Trabelsi, R., Zouari, K., and Daniele, S., 2017. Integrated socio-hydrogeological approach to tackle nitrate contamination in groundwater resources. The case of Grombalia Basin (Tunisia). *Science of The Total Environment*,

593-594, p.664-676. DOI:10.1016/j.scitotenv.2017.03.151.

Rositha, S.A., Ista'la, M.A.C., Ramadhan, G.R., and Muzakky, M.A., 2024. Geology and Economic Potential of Pyrophyllite Deposits in Argotirto Village, Sumbermanjing Wetan District, Malang Regency, East Java Province. *PIT IAGI Balikpapan 2024*. https://www.researchgate.net/publication/385812130.

Rout, C. and Setia, B., 2018. Assessment of groundwater quality for suitability of industrial purposes Constriction scour View project Assessment of Groundwater quality of N-E Haryana View project. *International Research Journal of Environmental Sciences*. https://www.researchgate.net/publication/325055862.

Ruiz-Pico, Á., Pérez-Cuenca, Á., Serrano-Agila, R., Maza-Criollo, D., Leiva-Piedra, J., and Salazar-Campos, J., 2019. Hydrochemical characterization of groundwater in the Loja Basin (Ecuador). *Applied Geochemistry*, 104, p.1-9. DOI:10.1016/j.apgeochem.2019.02.008.

Salami, S.A. and Akperi, O.G., 2023. Hydrogeochemical Assessment of Groundwater Quality and Geological Influence in Igarra and environs, Southwestern Nigeria. *Journal of Applied Sciences and Environmental Management*, 27 (4), p.853-861. DOI:10.4314/jasem.v27i4.30.

Schoeller, H., 1977. *Geochemistry of Groundwater. In: Groundwater Studies—An International Guide for Research and Practice*. UNESCO, Paris.

Sefie, A., Aris, A.Z., Shamsuddin, M.K.N., Tawnie, I., Suratman, S., Idris, A.N., Saadudin, S.B., and Wan Ahmad, W.K., 2015. Hydrogeochemistry of Groundwater from Different Aquifer in Lower Kelantan Basin, Kelantan, Malaysia. *Procedia Environmental Sciences*, 30, p.151-156. DOI:10.1016/j.proenv.2015.10.027.

Setiawan, T., Syah Alam, B.Y., Haryono, E., and Hendarwan, 2020. Hydrochemical and environmental isotopes analysis for characterizing a complex karst hydrogeological system of Watuputih area, Rembang, Central Java, Indonesia. *Hydrogeology Journal*, 28, p. 1635-1659. DOI:10.1007/s10040-020-02128-8.

Siddha, S. and Sahu, P., 2022. Evaluation of corrosivity and scaling properties of groundwater of Central Gujarat for industrial usage. *Arabian Journal of Geosciences*, 15 (9), 15pp. DOI:10.1007/s12517-022-10197-0.

Singh, K.K., Tewari, G., and Kumar, S., 2020. Evaluation of Groundwater Quality for Suitability of Irrigation Purposes: A Case Study in the Udham Singh Nagar, Uttarakhand. *Journal of Chemistry*, 2020. DOI:10.1155/2020/6924026.

Soro, T.D., Soro, G., Ahoussi, K.E., Oga, Y.M.S., and Soro, N., 2019. Hydrogeochemical and Groundwater Quality Studies in the High Bandama Watershed at Tortiya (Northern of Cand#244;te d'Ivoire). *Journal of Geoscience and Environment Protection*, 07 (02), p.49-61. DOI:10.4236/gep.2019.7200.4.

Sridharan, M. and Senthil Nathan, D., 2017. Groundwater quality assessment for domestic and agriculture purposes in Puducherry region. *Applied Water Science*, 7 (7), p.4037-4053. DOI:10.1007/s13201-017-0556-y.

Suhendar, R., Hadian, M.S.D., Muljana, B., Setiawan, T., and Hendarwan, 2020. Geochemical Evolution and Groundwater Flow System in Batujajar Groundwater Basin Area, West Java, Indonesia. *Indonesian Journal on Geoscience*, 7 (1), p.87-104. DOI: 10.17014/ijog.7.1.87-104

Sukadana, I. and Indrastomo, F.D., 2011. Kombinasi Pengukuran Radioaktivitas Batuan Dan Geolistrik Dalam Menentukan Akuifer Air Tanah Potensial Di Desa Sumbermanjing Kulon, Pagak, Malang, Jawa Timur. *Eksplorium*, 32 (2), p.125-138.

Sun, W. and Liu, Z., 2023. Third-Party Governance of Groundwater Ammonia Nitrogen Pollution: An Evolutionary Game Analysis

Considering Reward and Punishment Distribution Mechanism and Pollution Rights Trading Policy. *Sustainability*, 15 (11), 16pp. DOI:10.3390/su15119091.

Taufiq, A., Hosono, T., Ide, K., Kagabu, M., Iskandar, I., Effendi, A.J., Hutasoit, L.M., and Shimada, J., 2018. Impact of excessive groundwater pumping on rejuvenation processes in the Bandung basin (Indonesia) as determined by hydrogeochemistry and modeling. *Hydrogeology Journal*, 26 (4), p.1263-1279. DOI:10.1007/s10040-017-1696-8.

Thin, P.P., Hendrayana, H., Wilopo, W., and Kawasaki, S., 2018. Assessment of groundwater facies in Wates Coastal Area, Kulon Progo, Yogyakarta, Indonesia. *Journal of Degraded and Mining Lands Management*, 5 (4), p.1389-1401. DOI:10.15243/jdmlm.2018.054.1389.

Tiwari, K.K., Krishan, G., Anjali, Prasad, G., Mondal, N.C., and Bhardwaj, V., 2020. Evaluation of fluoride contamination in groundwater in a semi-arid region, Dausa District, Rajasthan, India. *Groundwater for Sustainable Development*, 11. DOI:10.1016/j.gsd.2020.100465.

Tóth, Á., Baják, P., Szijártó, M., Tiljander, M., Korkka-Niemi, K., Hendriksson, N., and Mádl-Szőnyi, J., 2023. Multimethodological Revisit of the Surface Water and Groundwater Interaction in the Balaton Highland Region—Implications for the Overlooked Groundwater Component of Lake Balaton, Hungary. *Water*, 15 (6), 27pp. DOI:10.3390/w15061006.

Utama, L.N.S., Rachmawati, T.A., and Hadisusanto, N., 2020. Penguluran River Flood Mitigation Strategy in Gedangan and Sumbermanjing Wetan Districts, Malang Regency. *Jurnal Sumberdaya Alam Dan Lingkungan*, 7 (1), 9pp. DOI:10.21776/ub.jsal.2020.007.01.2.

Vasilache, N., Vasile, G.G., Diacu, E., Modrogan, C., Paun, I.C., and Pirvu, F., 2020. Groundwater quality assessment for drinking and irrigation purpose using GIS, Piper diagram, and water quality index. *Romanian Journal of Ecology and Environmental Chemistry*, 2 (2), p.109-117. DOI:10.21698/rjeec.2020.214.

Weight, W.D., 2008. *Hydrogeology Field Manual*.

Wilopo, W., Putra, D.P.E., and Susatio, R., 2020. Aquifer distribution and groundwater geochemistry in bojonegoro sub-district, bojonegoro district, east java province, Indonesia. *Journal of Degraded and Mining Lands Management*, 7 (4), p.2327-2335. DOI:10.15243/jdmlm.2020.074.2327.

Xie, H., Li, J., and Liu, D., 2021. Characteristics and traceability analysis of nitrate pollution in the Yellow River Delta, China. *IOP Conference Series: Earth and Environmental Science*, 821 (1), 7pp. DOI:10.1088/1755-1315/821/1/012020.

Xu, W. and Su, X., 2019. Challenges and impacts of climate change and human activities on groundwater-dependent ecosystems in arid areas – A case study of the Nalenggele alluvial fan in NW China. *Journal of Hydrology*, 573, p.376-385. DOI:10.1016/j.jhydrol.2019.03.082.

Yan, J., Chen, J., and Zhang, W., 2021. Study on the groundwater quality and its influencing factor in Songyuan City, Northeast China, using integrated hydrogeochemical method. *Science of the Total Environment*, 773. DOI:10.1016/j.scitotenv.2021.144958.

Yuan, J., Li, Q., and Zhao, Y., 2022. The research trend on arsenic pollution in freshwater: a bibliometric review. *Environmental Monitoring and Assessment*, 194 (9), 18pp. DOI:10.1007/s10661-022-10188-4.

Yuwanto, S.H. and Ridwan, M., 2017. Studi Zona Alterasi Daerah Argotirto Dan Sekitarnya, Kecamatan Sumbermanjing Wetan, Kabupaten Malang, Provinsi Jawa Timur. *Seminar Nasional Sains Dan Teknologi Terapan V*.

Zamroni, A., Trisnaning, P.T., Prasetya, H.N.E., Sagala, S.T., and Putra, A.S., 2022. Geochemical Characteristics and Evaluation of the Groundwater and Surface Water in

Limestone Mining Area around Gunungkidul Regency, Indonesia. *Iraqi Geological Journal*, 55 (1), p.190-199. DOI:10.46717/igj.55.1E.15Ms-2022-05-31.

Zhang, Q., Xu, P., and Qian, H., 2019. Assessment of Groundwater Quality and Human Health Risk (HHR) Evaluation of Nitrate in the. *International Journal of Environmental Research and Public Health Article*.

Zhi, C., Cao, W., Zhang, Z., Li, Z., and Ren, Y., 2021. Hydrogeochemical characteristics and processes of shallow groundwater in the yellow river delta, china. *Water (Switzerland)*, 13 (4), 14pp. DOI:10.3390/w13040534.